Japanese Journal of Applied Physics
Vol. 47, No. 12, 2008, pp. 8752–8755

Shot Noise Suppression in SiGe Resonant Interband Tunneling Diodes

Youngsang KIM, Hyunwook SONG[1], Takhee LEE[1], and Heejun JEONG*

Department of Applied Physics, Hanyang University, Ansan 426-791, Korea
[1]*Department of Materials Science and Engineering, Gwangju Institute of Science and Technology, Gwangju 500-712, Korea*

(Received August 27, 2008; revised September 16, 2008; accepted September 19, 2008; published online December 19, 2008)

We report experimental noise studies of SiGe resonant interband tunneling diodes (RITDs) to probe the tunneling transport properties. The shot noise measurements show the signatures of coherent transport not only in the positive differential resistance (PDR) region but also in the plateau-like region on the negative differential resistance (NDR) side of the current–voltage (I–V) trace. The experimentally extracted Fano factor $F < 0.5$ may suggest that the coherent transport gradually becomes obvious in the NDR region. The variation of the Fano factor through the resonance process is discussed according to the recent theoretical model of coherent tunneling. [DOI: 10.1143/JJAP.47.8752]

KEYWORDS: SiGe, RITD, shot noise, coherent transport

1. Introduction

The advances in epitaxial technologies like molecular beam epitaxy, chemical vapor deposition, etc., enabled fabrication of semiconductor heterostructures. The large portion of works has been focused on the GaAs/AlGaAs based III–V compounds and the quantum well structures realized in this heterostructures have provided model systems for observing diverse quantum mechanical phenomena.[1–3] On the other hand, SiGe based devices are considered highly desirable due to the compatibility with the mainstream Si complementary metal–oxide–semiconductor (CMOS) technology.[4,5] Recently, SiGe RITDs were investigated as a basic unit of a low voltage monostable bistable transition logic gate (MOBILE)[6] and a vertically integrated heterobipolar transistor (HBT).[4] The RITD device structures were originally proposed by Sweeny *et al.*,[7] and experimentally realized by Rommel *et al.*[8] In this paper, we report our experimental investigation of the transport properties in SiGe RITD devices carried out by the analysis of the current noise characteristics.

The low-frequency noise measurements have recently been employed to study the suppression as well as the enhancement of shot noise with respect to the "full" shot noise value of $2e|I|$, where $q = e$ is the electron charge and I is the average current through the device.[9] If individual electrons are transmitted randomly from one side to the other, as in vacuum diodes, noise is Poissonian, having a frequency independent spectral density $S_I = 2e|I|$. Correlation between electrons would make an influence on randomness and therefore affect the shot noise characteristics. The few results available in the negative differential resistance (NDR) region exhibit a behavior very different from the shot noise suppression found in the positive differential resistance (PDR) region.[10] The noise suppression is expected to be greatest when the two barriers of resonant tunneling diodes (RTDs) have equal transmission coefficients and it was claimed that the Fano factor F can be as low as 0.5.[11] The shot noise suppression is due to the Pauli exclusion principle and Coulomb interaction between charged particles. In the coherent tunneling regime, there is no electron scattering during the electron transmission through the double-barrier structure.[12] Likewise, electron transport is governed by the total transparency of the tunneling barrier. By contrast, in the sequential tunneling regime, electrons scatter inside the quantum well.[13] Electrons tunnel through each barrier independently, so the scattering destroys the coherence. If we consider only current–voltage (I–V) characteristics, it is not possible to distinguish between these two transport regimes and naturally the question whether the tunneling transport is coherent or sequential remains unsolved.[14] Shot noise measurement provides a chance to distinguish the sequential and coherent tunneling phenomena in RTDs.

2. Experimental Procedure

The RITD employed in our measurement has the layer sequence of 10 Å p+ $Si_{0.4}Ge_{0.6}$/B δ-doped Si/40 Å undoped $Si_{0.4}Ge_{0.6}$/60 Å undoped Si/P δ-doped and grown by low-temperature molecular beam epitaxy (LT-MBE), where the delta doped concentration is $10^{14}/cm^2$. A calculated band diagram of SiGe RITD is shown in Fig. 1(a). In order to measure the I–V curves, we used a ground isolated DAC source and a low noise current amplifier. Differential conductance curves including d^2I/dV^2 were recorded with SR830 lock-in amplifier using an AC modulation of $100\,\mu V_{rms}$ amplitude with a frequency of 1.333 kHz. In practice, the noise of the numerical derivatives is much larger than the measured derivative terms. For the measurement of shot noise the signal from the RITDs was first amplified with a gain of 10 or 100 by two parallel sets of SR560 low-noise voltage amplifiers at room temperature. The noise spectrum was obtained by a cross correlation of the two individual amplifier signals using a SR780 dual channel spectrum analyzer. Calculation of the cross-correlation spectrum of the two detector outputs allows the removal of the uncorrelated voltage noise sources of the amplifiers containing a large $1/f$ component and the thermal noise of the leads. The cross spectra were averaged 5,000 times, which takes about 1 min, between 128 Hz to 102.4 kHz. Because the noise level we are expecting was on the order of $nV/\sqrt{Hz}$ all the grounds were isolated to remove ground-loops and samples were shielded carefully against RF interference at low temperature. Before continuing the measurement of the noise from RITD, it is necessary to calibrate in detail about the characteristics of the measurement setup to carry out proper data analysis on the measured data. There is a RC-damping of the measured signal because the whole measurement setup behaves like a

*E-mail address: hjeong@hanyang.ac.kr

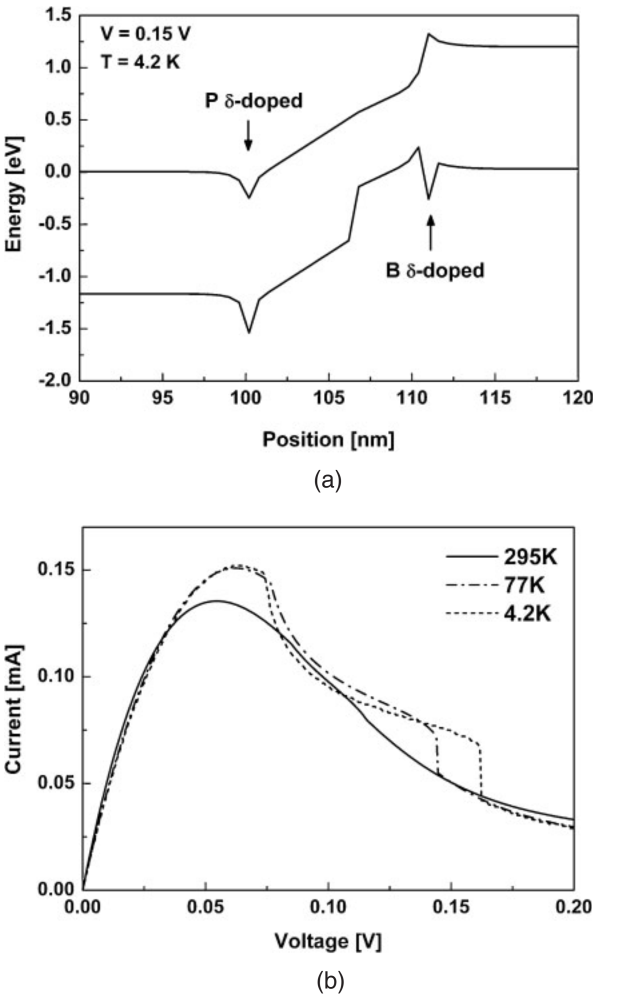

Fig. 1. (a) Calculated band diagram of the SiGe RITD using Poisson's equation. The δ-doping provides quantum wells for each band. (b) *I–V* characteristics of a RITD at room temperature, 77 K, and 4.2 K. Under low temperature, the plateau-like structures are observable because of both the localization of the confining potential at the emitter quantum well as a result of the constructive interference of the incident and the reflected electron waves and the coupling between energy levels in the emitter side well and in the other side well on account of the wave function overlap around the plateau-like regime.

RC-filter with the total resistance R and the total capacitance C of all the measurement lines and amplifiers. This attenuation can be calibrated by measuring the equilibrium Johnson-Nyquist voltage noise $S_V = 4k_BRT$ as a function of temperature T, where k_B is the Boltzmann constant and R is the sample resistance. The calibration was checked for different frequencies and sample resistances. The voltage gain as well as the offset in the voltage noise $S_I^{\text{off}} \cdot R_{\text{diff}}^2$ caused by the finite current noise S_I^{off} of the system can be determined with high accuracy, where R_{diff} is a differential resistance. The current noise S_I was finally obtained from the measured voltage fluctuations by $S_I = S_I^{\text{T}} - 4k_BTg - S_I^{\text{off}}$, where $g = dI/dV_{\text{SD}}$ is the bias-dependent differential conductance, where S_I^{T} is the total current noise as a function of the source–drain bias applied to RITD. After measurement calibration, the cross-correlation spectra were obtained with changing DC bias voltages applied to the sample, and finally, we obtained the current shot noise S_I as a function of frequency. A convenient quantity to measure the shot noise deviation from the Poissonian value is the Fano factor F,

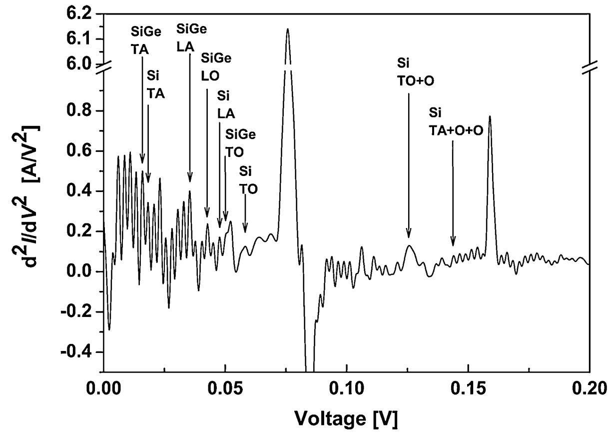

Fig. 2. Four well-defined peaks of SiGe alloy and five peaks of Si are observed in the second derivative spectra which correspond to the energy of TA, LA, LO, TO, TO+O, and TA+O+O (see ref. 20). This spectrum is obtained with the second-harmonic lock-in technique at 4.2 K.

defined as the ratio between the actual shot noise S_I and $2e|I| = 2eGV$, where $|I|$ is the average current and G is the differential conductance.[15)]

3. Results and Discussion

The *I–V* curves for a RITD are shown in Fig. 1(b). As a characteristic feature, under the forward bias, the peak current I_P at low temperatures is higher than that at room temperature. I_P grows from 135 to 152 μA, and simultaneously the valley current I_V falls from 27 μA to 15 μA, which finally produces a large change of the peak-to-valley current ratio (PVCR) γ (from $\gamma \approx 5$ to 10) for room temperature and 4.2 K, respectively. The *I–V* curves at 77 and 4.2 K show a clearly developed plateau-like structure which is not obvious at room temperature.[16)] Also, the width of the plateau-like structure increases as the temperature goes down. Buot *et al.*[17)] and Zhao *et al.*[18)] claimed that an emitter quantum well (EQW) was formed after the bias voltage swept over the resonance position and the characteristic plateau-like structure was attributed to the coupling between the quantized emitter energy levels and the level inside the other side well. A recent experimental observation by Qiu *et al.*[19)] supports these approaches.

The second derivative of the *I–V* curve, d^2I/dV^2, in Fig. 2, has been used to detect weak nonlinear signals, such as phonon-assisted electron tunneling through a barrier at very low temperature. Phonon spectroscopy provides a better understanding of the mechanism that limits the transport of heat or electrical charge inside tunneling devices. As the bias voltage is increased, the four well-defined peaks of SiGe alloy and five peaks of Si are observed which correspond to the energies of four fundamental phonons, the transverse acoustic (TA), the longitudinal acoustic (LA), the longitudinal optic (LO), the transverse optic (TO), the transverse optic combination (TO+O), and the three phonon combination (TA+O+O).[20)] We regard the strong peaks around 80 and 160 mV are due to the oscillation characteristics of the *I–V* curve. With the measurement of phonon spectroscopy, we can imagine that the small extra peaks reflect the existence of additional states due to the defect or other substances. The relative smallness of the peak strength of them suggests that they do not play a crucial role

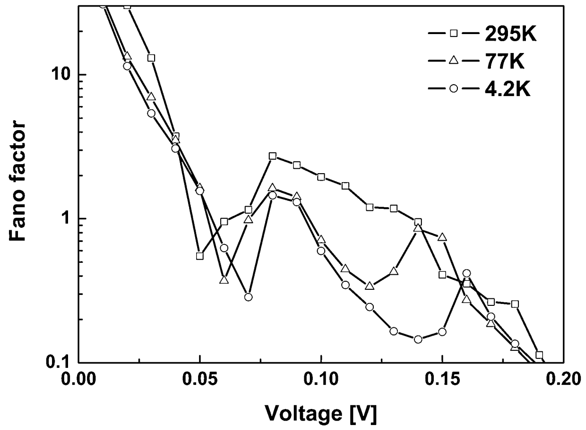

Fig. 3. Fano factor F as a function of bias voltage. Fano factor at low temperature is more dropped than room temperature in the NDR region. The minimum Fano factors around current peak regimes are 0.55, 0.37, and 0.29 for room temperature, 77 K, and 4.2 K, respectively. The Fano factor drops again strongly under 0.5 around the plateau-like regime.

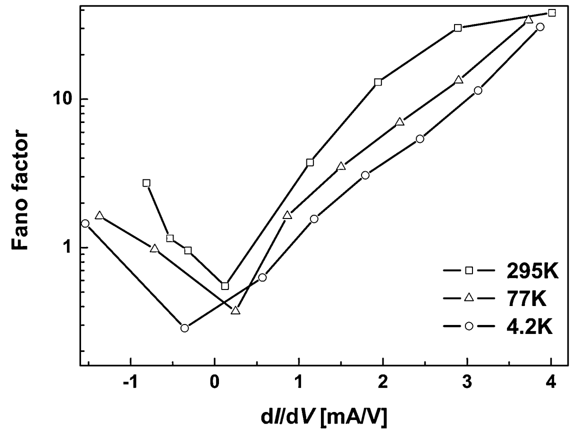

Fig. 4. Fano factor F as a function of differential conductance of the SiGe RITD demonstrates the coherent transports both in the current peak regime and in the plateau-like regime which have differential conductance between -1 and $+1$ mA/V. Both regimes show the shot noise suppression.

in the conduction. The clear second-order derivative signal is a good example of confirming the high sensitivity of our measurement circuitry.

Figure 3 shows the Fano factor F as a function of bias voltage by using shot noise measurement. The minimum Fano factor around NDR regime is 0.55, 0.37, and 0.29 for room temperature, 77, and 4.2 K, respectively. It is widely accepted that the Pauli exclusion and the charge interaction are the two correlation effects, which cause observed shot noise deviation from the full value. While the Pauli exclusion always causes shot noise suppression, the charge correlation may suppress or enhance the noise, depending on the conduction regime. In RTDs, it was experimentally found that the noise is partially suppressed (sub-Poissonian noise $F < 1$) in PDR region and enhanced (super-Poissonian, $F > 1$) in the negative differential conductance (NDC) region.[21] Aleshkin *et al.*[22] recently claimed that while in the sequential tunneling regime Fano factor F is still limited by the lowest value of 0.5, Fano factor F may drop below the value of 0.5 in the coherent tunneling regime. The overall observed tendency of the Fano factor below the value of 0.5 in our observation seems supporting the coherent tunneling model. An interesting feature is the double peak structure of the Fano factor in the NDR region. The position of the first peak and that of the second one coincide with the edges of the plateau-like region in the I–V curve. The shot noise measurements in the plateau regime in RTDs have been carried out very few times although there were many shot noise experiments regarding the resonant tunneling. Recently, the comparison of coherent tunneling and sequential tunneling model in RTD structures has been studied theoretically.[22] In that work, a double peak structures in coherent case were demonstrated even the authors did not mention the physical origin, which is different from the sequential case. The emergence of a double peak in the theoretical calculations might be a coincidence, even if they carry the coherent characteristics. The increasing feature of the Fano factor can be explained by the effect of Coulomb interaction resulting in the lifted potential in the well.[23] Just after the resonance peak position, charging of the quantum well raises the level inside, which means the wave function overlap between the emitter side and the energy level in the well is maintained even by increasing the bias voltage. In our case, we notice the correlation between the Fano factor peak position and the plateau edges. As is well known, the origin of the plateau region is the emitter quantization effect by the formation of quasi-quantum well in the emitter interface by applying bias voltage. We believe that the consecutive emergence of quantized levels in the emitter side and their coupling to the level in the other electrode side is manifested as a multiple peak structure of the Fano factor in our RITD device. Hence, our observation is another way of verifying the formation of the multiple energy level coupling through the shot noise measurement.

Another feature in our data is the further decreasing tendency of the Fano factor in higher bias region. Based on a simple conjecture, we can image that the carrier temperature increases as the bias voltage increases. The average energy gained by carriers in the well through the randomizing by interactions between carriers will also be increased resulting in higher carrier temperature than the lattice. In this situation, the carrier distribution is more probable to follow Boltzmann distribution, which means the Pauli exclusion principle becomes less significant. Then there is more possibility to observe the increase of the Fano factor rather than the decrease shown in our data. Currently we do not have clear understanding of this feature in the high bias region. There is another theoretical interpretation that the spin–orbit coupling effect can lead to shot noise suppression below the value of 0.5.[24] In our case, the relative smallness of the spin–orbit coupling (SOC) strength for SiGe compared to GaAs or other materials systems may give less significant result.

We demonstrate intuitive analysis by the conductance measurement in Fig. 4. As the conductance increases, the shot noise is gradually stronger. Under the regime of low differential conductance between -1 and $+1$ mA/V, the noise shows the sub-Poissonian process and the coherent transport. Likewise, we may think the change of current flux makes electronic fluctuation or scattering increase with breaking coherence. We estimate both electronic fluctuation and energy loss decrease with low thermal energy in the constant current regime.

4. Conclusions

In this paper, we have demonstrated the tunneling properties of SiGe RITDs by means of temperature dependent electronic transport, tunneling spectroscopy and shot noise characteristics. The PVCR γ is increased twice at 4.2 K than the PVCR at room temperature (from $\gamma \approx 5$ to 10). The Fano factor F at 4.2 K is more dropped to the value of 0.29 than the Fano factor $F = 0.55$ at room temperature around the resonant tunneling regime. The experimentally observed double peak structure of Fano factor in low temperature may suggest that the coherent tunneling is a dominant process in NDR region of RTDs. The experimental approach with shot noise measurement provides us a chance to distinguish the sequential and coherent tunneling phenomena in the electron transport in SiGe RITDs.

Acknowledgment

This work was supported by the Korea Research Foundation Grant funded by the Korean Government (MOEHRD, KRF-2008-331-C00107).

1) Swaroop Ganguly, L. F. Register, S. Banerjee, and A. H. MacDonald: Phys. Rev. B **71** (2005) 245306.
2) Y. Chen and R. A. Webb: Phys. Rev. B **73** (2006) 035424.
3) A. Ben Simon, Y. Paltiel, G. Jung, V. Berger, and H. Schneider: Phys. Rev. B **76** (2007) 235308.
4) S.-Y. Chung, N. Jin, P. R. Berger, R. Yu, P. E. Thompson, R. Lake, S. L. Rommel, and S. K. Kurinec: Appl. Phys. Lett. **84** (2004) 2688.
5) K.-J. Gan, C.-S. Tsai, D.-S. Liang, C.-M. Wen, and Y.-H. Chen: Jpn. J. Appl. Phys. **45** (2006) L977.
6) U. Auer, W. Prost, M. Agethen, F. J. Tegude, R. Duschl, and K. Eberl: IEEE Electron Device Lett. **22** (2001) 215.
7) M. Sweeny and J. Xu: Appl. Phys. Lett. **54** (1989) 546.
8) S. L. Rommel, T. E. Dillon, M. W. Dashiell, H. Feng, J. Kolodzey, P. R. Berger, P. E. Thompson, K. D. Hobart, R. Lake, A. C. Seabaugh, G. Klimeck, and D. K. Blanks: Appl. Phys. Lett. **73** (1998) 2191.
9) Ya. M. Blanter and M. Büttiker: Phys. Rep. **336** (2000) 1.
10) V. V. Kuznetsov, E. E. Mendez, J. D. Bruno, and J. T. Pham: Phys. Rev. B **58** (1998) R10159.
11) J. H. Davies, P. Hyldgaard, S. Hershfield, and J. W. Wilkins: Phys. Rev. B **46** (1992) 9620.
12) L. L. Chang, L. Esaki, and R. Tsu: Appl. Phys. Lett. **24** (1974) 593.
13) S. Luryi: Appl. Phys. Lett. **47** (1985) 490.
14) A. K. M. Newaz, W. Song, E. E. Mendez, Y. Lin, and J. Nitta: Phys. Rev. B **71** (2005) 195303.
15) C. W. J. Beenakker and M. Buttiker: Phys. Rev. B **46** (1992) 1889.
16) K. Shinohara, S. Shimonura, and S. Hiyamzi: Jpn. J. Appl. Phys. **38** (1999) 5037.
17) F. A. Buot, P. Zhao, H. L. Cui, D. L. Woolard, K. L. Jensen, and C. M. Krowne: Phys. Rev. B **61** (2000) 5644.
18) P. Zhao, H. L. Cui, and D. L. Woolard: Phys. Rev. B **63** (2001) 075302.
19) Z. J. Qui, Y. S. Gui, S. L. Guo, N. Dai, J. H. Chu, X. X. Zhang, and Y. P. Zeng: Appl. Phys. Lett. **84** (2004) 1961.
20) R. A Logan, J. M. Rowell, and F. A. Trumbore: Phys. Rev. **136** (1964) A1751.
21) V. Nam Do, P. Dollfus, and V. Lien Nguyen: J. Appl. Phys. **100** (2006) 093705.
22) V. Y. Aleshkin, L. Reggiani, and M. Rosini: Phys. Rev. B **73** (2006) 165320.
23) G. Iannaccone, G. Lombardi, M. Macucci, and B. Pellegrini: Phys. Rev. Lett. **80** (1998) 1054.
24) R. Zhu and Y. Guo: Appl. Phys. Lett. **90** (2007) 232104.